Journal of Dental Sciences 20 (2025) 147–153

Available online at www.sciencedirect.com

ScienceDirect

journal homepage: www.e-jds.com

Original Article

High-precision and non-invasive measurement of crestal bone level by optical coherence tomography

Wei-Ting Chang [a,b], Dong-Yuan Lyu [a], Yu-Lin Lai [a,b], Jui-Ying Yen [b,c], Ya-Chi Chen [a,b], Shyh-Yuan Lee [a,b,c,d*]

[a] School of Dentistry, National Yang Ming Chiao Tung University, Taipei, Taiwan
[b] Department of Stomatology, Taipei Veterans General Hospital, Taipei, Taiwan
[c] Department of Dentistry, Yangming Branch of Taipei City Hospital, Taipei, Taiwan
[d] Oral Medicine Innovation Center, National Yang Ming Chiao Tung University, Taipei, Taiwan

Received 6 August 2024; Final revision received 13 September 2024
Available online 27 September 2024

KEYWORDS
Diagnostic imaging;
Optical coherence tomography;
Periodontium;
Crestal bone level

Abstract *Background/purpose:* Identifying crestal bone level (CBL) on the buccal and lingual aspects poses challenges in conventional dental radiographs. Given that optical coherence tomography (OCT) has the capability to non-invasively provide in-depth information about the periodontium, this in vitro study aimed to assess whether OCT can effectively identify periodontal landmarks and measure CBL in the presence of gingiva.

Materials and methods: An in-house handheld scanning probe connected to a 1310-nm swept-source OCT (SS-OCT) system, along with self-developed algorithms were employed to measure the CBL in dental models with artificial gingiva. Markers were positioned 0.5 mm above the artificial gingival margin (SG) and the crestal bone (SC) on both the mid-buccal and mid-lingual sides of 28 plastic teeth. The distances between the paired SG and SC were measured in the OCT images after correcting for the optical path through the covering artificial gingiva. These measurements were subsequently compared to the ground truth values obtained using a 2.5D inspection system.

Results: The mean difference in CBL measured by SS-OCT and 2.5D was 0.008 mm (95 % CI: −0.092 to 0.108 mm). Statistical analysis using a three-way ANOVA indicated that the measurement differences were not significant across maxillary/mandible, anterior/posterior, and buccal/lingual dimensions. Furthermore, these differences were not associated with gingival thickness ($\alpha = 0.05$).

Conclusion: The proposed SS-OCT system demonstrated its capability to accurately and non-invasively assess CBL through artificial gingiva. Moreover, it facilitated the semi-automatic delineation of critical periodontal landmarks on OCT en face images, highlighting its potential for clinical applications.

* Corresponding author. School of Dentistry, National Yang Ming Chiao Tung University, No. 155, Sec. 2, Linong Street, Taipei, 112304, Taiwan.
E-mail address: sylee@nycu.edu.tw (S.-Y. Lee).

https://doi.org/10.1016/j.jds.2024.09.005

Introduction

Accurate and non-invasive measurement of crestal bone level (CBL) is essential for all dental treatments. Standardized periapical radiographs can reliably identify interproximal bone defects.[1] However, they encounter challenges when applied to the buccal and lingual aspects.[2] Transgingival probing could effectively detect bone levels by allowing the probe tip to penetrate through the gingival sulcus to the crestal bone,[3] however, its invasive nature limits its applicability. Recently, cone beam computed tomography (CBCT) has provided valuable information about bone in all directions around the teeth,[4,5] yet the high radiation dose makes it unsuitable for routine periodontal examinations.[6]

Currently, several innovative technologies have been proposed for assessing oral tissues at specific depths. Among these, optical coherence tomography (OCT) and ultrasonography stand out as the notable contenders. OCT, in particular, distinguishes itself as a promising tool for non-invasive, high-quality imaging in the field of oral diagnostics. It employs low-coherence interferometry to generate three-dimensional (3D) volumetric images of the internal microstructure of tissues.[7,8] This imaging technique has been applied to investigate dental caries,[9] tooth cracks,[10] and soft tissue cancers.[11] In periodontal diagnosis, it has revealed detailed structures such as the gingival epithelium, connective tissue, dental calculus, and alveolar bone.[8,12–17] Prior studies have validated the accuracy of OCT in measuring soft tissue thickness and gingival sulcus depth.[14,18] Notably, these studies implemented optical path correction to enhance measurement precision. Given that light deviates when transitioning between different media, optical path length discrepancies can be rectified by employing the refractive index of gingival tissue.[12,14,18–21]

While earlier OCT studies have demonstrated promising results in exploring delicate periodontal substructures, many of these investigations primarily offered conceptual information regarding periodontal assessment and often lacked well-controlled measurements.[12,14,18–21] Consequently, the true accuracy of using OCT to measure CBL remains unverified. Moreover, most studies have only presented single longitudinal image (B scans), which curtails the advantages of OCT for 3D volumetric imaging in clinical applications. Therefore, the purposes of this *in vitro* study were to validate the accuracy of OCT in measuring CBL using artificial models and to demonstrate the integration of OCT images to visualize CBL in periodontal topography. We hypothesized that OCT could effectively detect the subgingival profile through artificial gingiva and use optical path correction for precise measurements.

Materials and methods

In-house dental OCT system

The in-house OCT system used in this study was specifically designed for dental applications and comprised four main components: a swept-source OCT (SS-OCT), a handheld probe, a signal processing unit, and algorithms tailored for periodontal use (Fig. 1A). The SS-OCT was equipped with a swept laser light source (HSL-2100, Santec, Komaki, Aichi, Japan) that featured a central wavelength of 1310 nm and a bandwidth of 100 nm, operating at a scan rate of 20 kHz. The average output power of the system was 25.5 mW. The handheld probe featured an integrated sleeve and lens system designed for lateral viewing during intraoral data acquisition (Fig. 1B). The images produced illustrated the relationship between intensity and penetration depth, known as axial scans or A scans. A compilation of multiple A scans generated a longitudinal tomographic image, referred to as a B scan. The resolution of the B scan images was 0.03 mm per pixel for both the X and Y axes. This real-time OCT system was capable of capturing a series of 250 B scans in 1.25 s to create a region of interest measuring 7.2 × 7.2 mm. The developed algorithms facilitated image reading, noise reduction, and optical distortion correction in OCT images. Additionally, the software could generate 3D information from B scans and compile transverse and integrated images (C scans or en face) for interpretation and measurement.

Study model preparation

To ensure precise measurement with fixed markers, a set of Nissin dental models (PRO2002, Nissin Dental Products Inc., Kyoto, Japan) equipped with removable gingiva analogs and 28 artificial teeth was employed. Hexagonal metal-coated glitters (Gold 1502—1, I-Cheng, Taipei, Taiwan), measuring 200—250 μm in size, were affixed to the model as reference markers using dental adhesive (Scotchbond™ Universal Adhesive, 3 M ESPE, St. Paul, MN, USA). These markers were positioned 0.5 mm above the gingival margin (supragingival, SG) and 0.5 mm above the crestal bone (supracrestal, SC) on the mid-buccal and mid-lingual surfaces of each tooth. The markers were easily identifiable in both visual examinations and OCT images (Fig. 2).

Optical path correction

To determine the refractive index of artificial gingiva, a flat stainless-steel stick was partially inserted into the artificial gingival sulcus. By aligning the deflected shape of the subgingival part with the supragingival part on the B scan, the refractive index of artificial gingiva (1.40) was

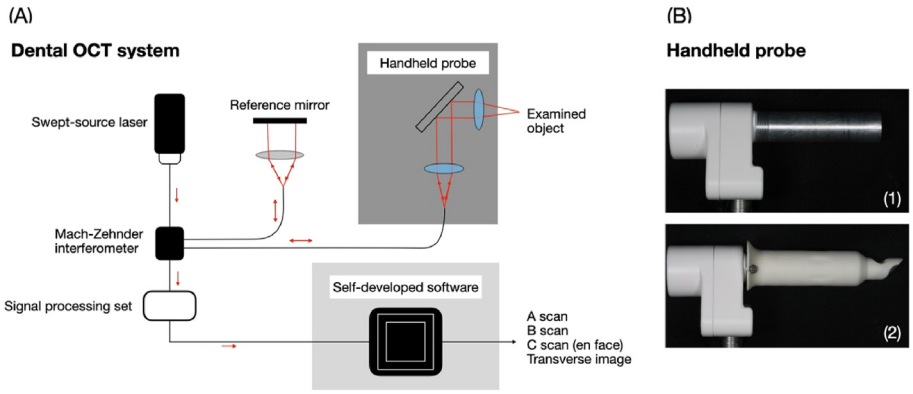

Figure 1 The dental OCT system and the handheld probe design. **A)** Schematic illustration of the components of the dental OCT system, including a swept source laser with a central wavelength of 1310 nm, Mach-Zehnder interferometer, a signal processing set, and self-developed software for periodontal application. **B)** The handheld probe (1) without a sleeve and (2) with a sleeve, which contains a lens system for side-viewing.

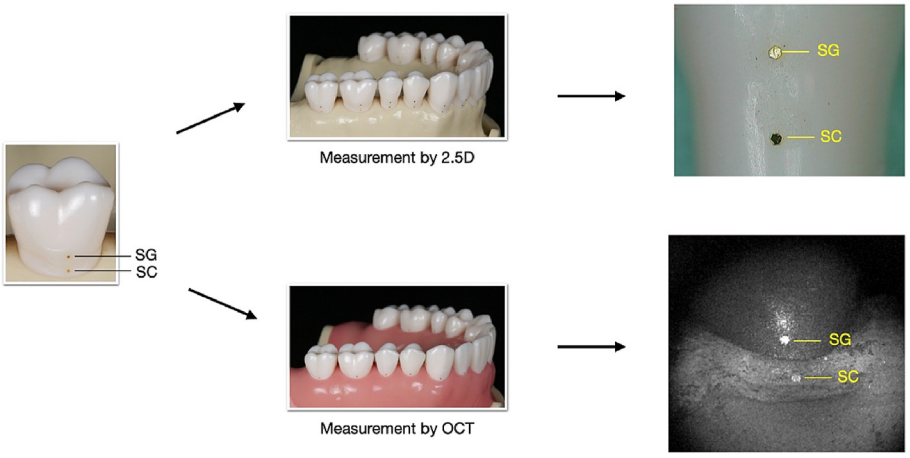

Figure 2 Illustrations of measurement markers and study design. The distances between SG and SC were measured by using both a 2.5D automatic vision measuring machine and OCT. SG = supragingival marker, SC = supracrestal marker.

extracted using a self-developed algorithm (Fig. 3). Thereafter, the algorithm was able to semi-automatically delineate the gingival region by detecting changes in signal intensity (Fig. 4B) and calibrating all B scans based on the provided refractive index.

Crestal bone level assessment

OCT images were captured from both the mid-buccal and mid-lingual sides of the artificial teeth in the presence of artificial gingiva. The distance between the crestal bone (SC) and the gingiva (SG), referred to as bone sounding depth, was measured on the calibrated B scans to evaluate the accuracy of OCT in assessing of CBL. The marker center was identified on the calibrated B scan and transverse images of OCT (Fig. 4A), and its spatial coordinates were used for distance calculations. To gain a better understanding of how the thickness of artificial gingiva affects the accuracy of CBL measurement, the gingival thickness at the SC level on each B scan was also measured (Fig. 4C).

For the intra-rater examination, 10 out of 56 sites on the models were randomly selected and measured three times by a single examiner (WT). For the inter-rater examination, a second examiner (DY) independently conducted measurements of the same sites, and the results were subsequently compared with those of the first examiner. Both intra- and inter-operator reliability of the measurements were assessed by calculating the intraclass correlation coefficient (ICC).

To verify the accuracy of measurements obtained with OCT, the distance between paired SG and SC at each site was directly measured using a 2.5D automatic vision measuring machine (AF3020, Nan Jie Co., Taichung, Taiwan), without the presence of artificial gingiva. This 2.5D machine featured an autofocus capability, ensuring a high measurement precision of 3 μm.

Clinical application

The clinical test was conducted in accordance with the Helsinki Declaration and received approval from the Institutional Review Board of National Yang Ming Chiao Tung University (YM110011F). To verify the applicability of the OCT system in a clinical setting, a buccal scan was performed on the left maxillary first molar of the author (WT).

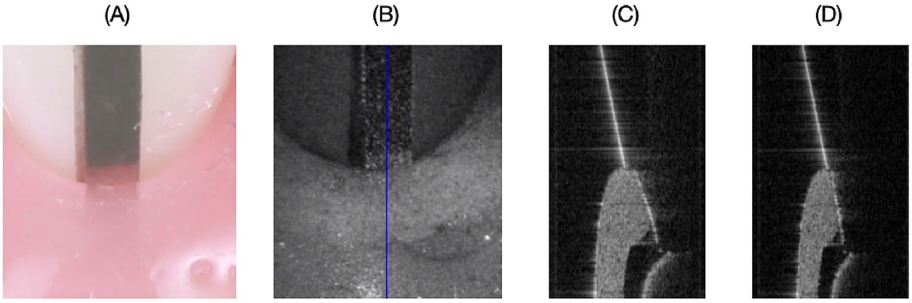

Figure 3 Optical path correction of artificial gingiva. **A)** The calibration metal stick partially inserted into the artificial gingival sulcus. **B)** The calibration stick in C scan. The B scan cut along the flat surface of the stick (blue line) was used for calibration. **C)** The calibration stick in the original B scan, where the metal surface beneath the artificial gingiva appeared distorted. **D)** The calibration stick in corrected B scan. The refractive index of the gingiva was determined when the metal surface beneath the artificial gingiva was realigned by applying 1.40 in the algorithm for optical path length correction.

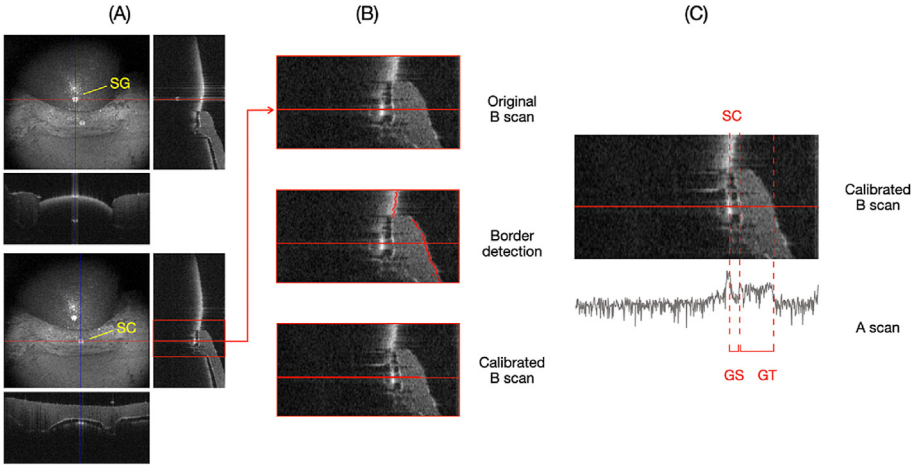

Figure 4 Measurement of crestal bone level and artificial gingival thickness. **A)** SG and SC in OCT images. The coordinates of the markers were identified in both B scan and transverse images. **B)** Calibrated B scan. The superficial border of the original B scan was semiautomatically detected by the algorithm, and optical path correction of artificial gingiva was performed by applying the refractive index of 1.40. **C)** Calibrated B scan displaying corresponding signal intensity of SC, GS, and GT in A scan. SG = supragingival marker; SC = supracrestal marker; GS = artificial gingival sulcus; GT = artificial gingival thickness.

Statistical analyses

All data analyses were conducted using IBM SPSS Statistics 24 (SPSS Inc., Chicago, IL, USA). The normal distribution and homogeneity of variance were assessed using the Shapiro–Wilk and Levene tests, respectively. Paired t-tests were employed to compare the CBL measurements obtained from OCT and the 2.5D machine. A three-way analysis of variance (ANOVA) was performed to evaluate the deviation of CBL measurements by the dental OCT system and the thickness of artificial gingiva across different examination sites (buccal/lingual, maxilla/mandible, anterior/posterior teeth). Additionally, the influence of gingival thickness on CBL measurements was assessed.

Results

Both the intra-rater and inter-rater assessments demonstrated excellent agreement, with high ICC scores of 0.986 and 0.952, respectively.

A total of 56 sites were examined for 28 artificial teeth. The mean distances between the SC and SG, as measured by the dental OCT system and the 2.5D machine, were 1.896 mm (95 % CI: 1.126 to 2.666) and 1.904 mm (95 % CI: 1.163 to 2.645), respectively. Both two measurement methods did not show a significant difference ($P > 0.05$) and exhibited a high correlation (0.992, $P < 0.05$) for each site. Compared to the reference value, the mean measurement error of the dental OCT system was 0.008 mm (95 % CI: −0.092 to 0.108) (Table 1). A three-way ANOVA indicated that different positional factors regarding maxillary/mandibular, buccal/lingual, and anterior/posterior did not have a significant effect on measurement errors ($P > 0.05$).

The mean thickness of the artificial gingiva at the SC level was 1.599 mm (95 % CI: 1.488 to 1.711). A statistically significant difference in artificial gingival thickness was observed between the anterior and posterior teeth ($P < 0.05$) (Table 1). However, the deviation of CBL measurement was not influenced by the gingival thickness.

Fig. 5 illustrates the periodontal profile of the left maxillary first molar, demonstrating the clinical

Table 1 Deviation of crestal bone level and gingival thickness measured by OCT at different locations.

	n	Deviation of crestal bone (mm)			Gingival thickness (mm)		
		Mean	95 % CI	*P*	Mean	95 % CI	*P*
Maxilla	28	−0.012	−0.110–0.086	0.984	1.564	1.066–2.062	0.616
Mandible	28	−0.004	−0.108–0.100		1.635	0.946–2.323	
Buccal	28	0.002	−0.093–0.096	0.085	1.638	1.009–2.267	0.270
Lingual	28	−0.019	−0.123–0.086		1.561	0.992–2.131	
Anterior	24	−0.008	−0.115–0.098	0.625	1.476	0.910–2.042	0.004[a]
Posterior	32	−0.009	−0.106–0.089		1.692	1.126–2.258	
Total	56	0.008	−0.092–0.108		1.599	1.488–1.711	

CI: confidence of interval.
[a] $P < 0.05$.

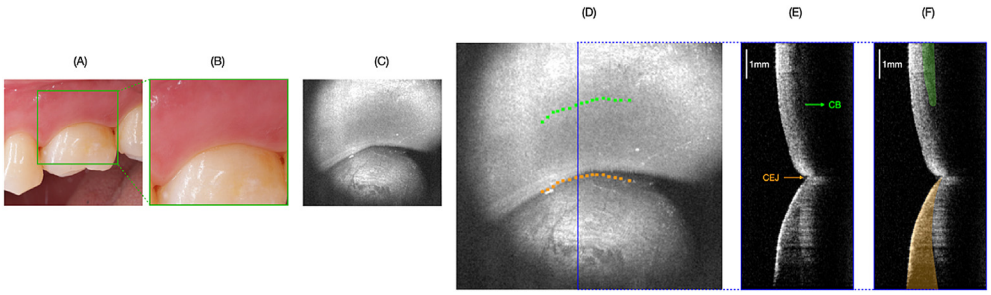

Figure 5 Establishing periodontal profiles of natural teeth in OCT. **A) & B)** Images of a human left maxillary first molar. **C)** Human maxillary first molar in C scan of OCT. **D)** Periodontal landmarks illustrated in C scan. **E &F)** The B scan from the plane of the blue line. Optical path correction was performed by the algorithm using a gingival refractive index of 1.40. CEJ = cervicoenamel junction; CB = crestal bone; green area: alveolar bone; yellow area: enamel.

applicability of the OCT system. In the presented B scan, optical path correction was implemented through artificial gingiva by applying a refractive index of 1.40. The en face image from the OCT, compiled from multiple B scans, highlights the identification of the cervicoenamel junction and crestal bone (Fig. 5).

Discussion

The applications of OCT in periodontal research have garnered significant attention. However, most studies have primarily focused on the conceptual advantages of OCT and have conducted measurements exclusively using two-dimensional B scan images.[12,14,18] In this study, we developed SS-OCT system that includes a handheld probe, enabling intraoral examinations. To our knowledge, this is the first study to demonstrate the accuracy of CBL measurements using OCT in a simulated full-mouth examination. Our results indicated that the mean deviation of the CBL measurements obtained from the proposed OCT system was only 0.008 mm, and this deviation was not affected by varying locations or gingival thicknesses in the study model. Furthermore, the system facilitated the visualization of periodontal landmarks through an algorithm applied to the en face OCT images (Fig. 5). These findings highlight the potential of the developed OCT system for future clinical studies.

Precise measurement of changes in bone level is crucial for the early diagnosis of periodontal and peri-implant diseases. The early stage of the disease, known as stage I periodontitis, is characterized by 1–2 mm of attachment loss. When assessing the rate of disease progression, periodontitis with rapid progression is defined as at least 2 mm of bone loss over a period of five years.[22] Detecting such difference in bone changes within a shorter observation period could be challenging with traditional tools. The average measurement errors for transgingival probing have been reported as 0.02 (±0.96 SD) mm and 0.12 (±0.92 SD) mm.[3,23] For radiographic tools, periapical radiographs have been reported to have a mean error of 0.27 (±1.26 SD) mm in bone level measurement, while the CBCT has an average error of 0.41 (±1.19 SD) mm.[5] Currently, the measurement deviation of CBL using ultrasonography can reach 0.078 mm (95 % CI: −0.952 to 0.797 mm).[24] In contrast, OCT emerges as an excellent candidate for detecting incipient bone defects and monitoring subtle bone changes. In the current study, the accuracy and precision of OCT were nearly 10-fold improved, enabling the detection of early and incipient lesions on both the buccal and lingual aspects.

The primary challenge in employing OCT for spatial distance measurements is in the deflection of light as it passes through different media. Consequently, a critical step in accurately measuring periodontal tissue with OCT is optical path correction. Variations in gingival thickness can result in varying degrees of distortion in OCT images, leading to errors in the assessment of crestal bone levels and gingival thickness. The refractive index of human gingiva has typically been determined using the extraoral

method, which involves measuring the optical path length of the gingiva in OCT images and dividing it by the actual thickness of the sectioned tissue.[25] Reports indicated that the gingival refractive indices obtained through the extraoral method are 1.39[14] and 1.40 for humans.[12,21] In contrast, the present study employed a non-invasive intraoral method[20] to retrieve the refractive index of artificial gingiva by correcting the shape deformation of a calibration stick on a B scan, yielding a value of 1.40, which is comparable to that of human gingiva (Fig. 4).

Theoretically, OCT can provide high-precision measurements. However, prior studies have shown inferior accuracy of OCT in measuring periodontal tissue, which might be due to the limitations of the comparison tools used.[12,21] While in this study, with the assistance of well-defined markers, OCT proved to be a highly precise and reliable modality for subgingival measurements, achieving high ICC scores for both intra-rater and inter-rater examinations. The mean deviation of 8 μm in this SS-OCT system is not only suitable for periodontal examinations, but also has the potential to be used for digital impressions of fixed dental prostheses with subgingival margins.

The identification of periodontal landmarks in the 3D reconstruction of OCT images can assist clinicians in visualizing tissue profiles.[14,19,26] In the present study, the algorithms employed were able to semiautomatically outline the gingival area across a series of B scans, and subsequently perform optical path correction for each scan. Furthermore, the spatial coordinates of the substructures could be virtually integrated for volumetric 3D reconstruction, significantly expanding the clinical applications of this technology (Fig. 5). Recent advancements have introduced convolutional neural network models and class activation maps for the automatic tracking of subgingival dental calculus.[16,17] These approaches hold promise for the automatic identification of periodontal landmarks in future studies.

The penetration depth of OCT may limit its clinical applications. In this study, the maximum penetration depth of the current OCT system in the artificial models was found to be 2.8 mm, whereas in human periodontium, it was decreased to 1.4 mm. Similar findings have indicated that the maximum penetration depths of OCT in human gingiva ranged from 1.2 to 1.5 mm, depending on factors such as central wavelength, incident light power, and the numerical aperture of the OCT system.[18,19,27,28] Clearly, the composition and condition of the target gingival tissue also significantly affect the penetration depth of the light. Central wavelengths of OCT between 1310 and 1330 nm are commonly used in dental applications.[12,14,19,27,28] Although the optical window between 1300 and 1400 nm is regarded as one of the most sensitive regions for biological imaging, the optimal wavelengths for periodontal examination have not yet been definitively established. Moreover, due to variations in tissue composition and condition, the wavelength required to achieved maximum penetration depth differs,[29] warranting further investigation.

In addition to the OCT technique, ultrasonography provides a non-invasive methods for observing the internal structure and measuring the thickness of the gingiva.[24,30,31] Ultrasonography has been utilized to assess gingival thickness during nonsurgical periodontal therapy,[32] guided tissue regeneration,[33] mucogingival therapy,[34,35] and implant treatment.[36] Although the signal penetration depth of ultrasonography surpasses that of OCT, its image resolution is inferior. Direct contact between the ultrasonic probe and the tissue may result in tissue compression, making the procedure more technique-sensitive and potentially causing discomfort for the patient.

The current investigation has demonstrated that OCT can be utilized for precise measurements. When conducting intraoral measurements with OCT, it is crucial to consider both the stability of the scanning head and the detection depth of OCT within the periodontal tissue. A stabilizer can be employed to ensure that the probe maintains close contact with the tissue during imaging. However, in patients with thicker gingival tissue, measuring the crestal bone level can pose challenges. A recent study reported that the average buccal gingival thickness among subjects from the Chinese population was 1.03 ± 0.31 mm,[37] as measured by transgingival probing. Based on previous OCT studies on human gingiva, its penetration depth can reach 1.2—1.5 mm,[18,19,27,28] suggesting that measuring CBL on the buccal aspect is generally feasible in most cases within this demographic.

In summary, within the constraints of this research, the 1310-nm dental SS-OCT system exhibited considerable accuracy in measuring CBL in vitro. Furthermore, it facilitated the visualization of intricate periodontal profiles through en face OCT imaging. The level of precision attained was submillimeter, underscoring its substantial potential for monitoring subtle alterations in bone surrounding teeth or implants. As an adjunct to conventional clinical and radiographic assessments, this pioneering noninvasive technology can furnish clinicians with critical insights to improve periodontal management. Consequently, further studies are highly recommended to elucidate the influence of oral conditions on the in vivo reliability of dental OCT.

Declaration of competing interest

Shyh-Yuan Lee and Dong-Yuan Lyu are co-inventors of the patent for the optical tomography digital impression system (US-104263468). The other authors declare that they have no conflicts of interest related to this article.

Acknowledgements

The study was supported in part by the National Science and Technology Council, Taiwan (Grant No. NSTC112-2218-E-A49-028-) and Department of Health, Taipei City Government (Grant No. 11001-62-034).

References

1. Grondahl K, Kullendorff B, Strid KG, Grondahl HG, Henrikson CO. Detectability of artificial marginal bone lesions as a function of lesion depth. A comparison between subtraction radiography and conventional radiographic technique. *J Clin Periodontol* 1988;15:156—62.
2. Lang NP, Hill RW. Radiographs in periodontics. *J Clin Periodontol* 1977;4:16—28.

3. Kim HY, Yi SW, Choi SH, Kim CK. Bone probing measurement as a reliable evaluation of the bone level in periodontal defects. *J Periodontol* 2000;71:729—35.
4. Scarfe WC, Farman AG. What is cone-beam CT and how does it work? *Dent Clin* 2008;52:707—30 [, v].
5. Misch KA, Yi ES, Sarment DP. Accuracy of cone beam computed tomography for periodontal defect measurements. *J Periodontol* 2006;77:1261—6.
6. Kim DM, Bassir SH. When Is Cone-Beam Computed Tomography Imaging Appropriate for diagnostic inquiry in the management of inflammatory periodontitis? An American Academy of Periodontology best evidence review. *J Periodontol* 2017;88:978—98.
7. Huang D, Swanson EA, Lin CP, et al. Optical coherence tomography. *Science* 1991;254:1178—81.
8. Colston B, Sathyam U, Dasilva L, Everett M, Stroeve P, Otis L. Dental OCT. *Opt Express* 1998;3:230—8.
9. Shimada Y, Sadr A, Burrow MF, Tagami J, Ozawa N, Sumi Y. Validation of swept-source optical coherence tomography (SS-OCT) for the diagnosis of occlusal caries. *J Dent* 2010;38:655—65.
10. Imai K, Shimada Y, Sadr A, Sumi Y, Tagami J. Noninvasive cross-sectional visualization of enamel cracks by optical coherence tomography in vitro. *J Endod* 2012;38:1269—74.
11. Gentile E, Maio C, Romano A, Laino L, Lucchese A. The potential role of in vivo optical coherence tomography for evaluating oral soft tissue: a systematic review. *J Oral Pathol Med* 2017;46:864—76.
12. Fernandes LO, Mota C, de Melo LSA, da Costa Soares MUS, da Silva Feitosa D, Gomes ASL. In vivo assessment of periodontal structures and measurement of gingival sulcus with optical coherence tomography: a pilot study. *J Biophot* 2017;10:862—9.
13. Otis LL, Everett MJ, Sathyam US, Colston Jr BW. Optical coherence tomography: a new imaging technology for dentistry. *J Am Dent Assoc* 2000;131:511—4.
14. Kakizaki S, Aoki A, Tsubokawa M, et al. Observation and determination of periodontal tissue profile using optical coherence tomography. *J Periodontal Res* 2018;53:188—99.
15. Tsubokawa M, Aoki A, Kakizaki S, et al. In vitro and clinical evaluation of optical coherence tomography for the detection of subgingival calculus and root cementum. *J Oral Sci* 2018;60:418—27.
16. Hsiao TY, Ho YC, Chen MR, Lee SY, Sun CW. Disease activation maps for subgingival dental calculus identification based on intelligent dental optical coherence tomography. *Translational Biophotonics* 2021;3:e202100001.
17. Hsiao TY, Ho YC, Lee SY, Sun CW. Degree of polarization uniformity for dental calculus visualization. *J Biophot* 2022:e202200011.
18. Park JY, Chung JH, Lee JS, Kim HJ, Choi SH, Jung UW. Comparisons of the diagnostic accuracies of optical coherence tomography, micro-computed tomography, and histology in periodontal disease: an ex vivo study. *J Periodontal Implant Sci* 2017;47:30—40.
19. Mota CC, Fernandes LO, Cimoes R, Gomes AS. Non-invasive periodontal probing through Fourier-domain optical coherence tomography. *J Periodontol* 2015;86:1087—94.
20. Kim SH, Kang SR, Park HJ, Kim JM, Yi WJ, Kim TI. Improved accuracy in periodontal pocket depth measurement using optical coherence tomography. *J Periodontal Implant Sci* 2017;47:13—9.
21. Fernandes LO, Mota C, Oliveira HO, Neves JK, Santiago LM, Gomes ASL. Optical coherence tomography follow-up of patients treated from periodontal disease. *J Biophot* 2019;12:e201800209.
22. Tonetti MS, Greenwell H, Kornman KS. Staging and grading of periodontitis: framework and proposal of a new classification and case definition. *J Periodontol* 2018;89(Suppl 1):S159—72.
23. Ursell MJ. Relationships between alveolar bone levels measured at surgery, estimated by transgingival probing and clinical attachment level measurements. *J Clin Periodontol* 1989;16:81—6.
24. Tattan M, Sinjab K, Lee E, et al. Ultrasonography for chairside evaluation of periodontal structures: a pilot study. *J Periodontol* 2020;91:890—9.
25. Hariri I, Sadr A, Shimada Y, Tagami J, Sumi Y. Effects of structural orientation of enamel and dentine on light attenuation and local refractive index: an optical coherence tomography study. *J Dent* 2012;40:387—96.
26. Lai YC, Chiu CH, Cai ZQ, et al. OCT-based periodontal inspection framework. *Sensors (Basel)* 2019;19:5496.
27. Otis LL, Colston Jr BW, Everett MJ, Nathel H. Dental optical coherence tomography: a comparison of two in vitro systems. *Dentomaxillofacial Radiol* 2000;29:85—9.
28. Wang LV, Wu H-i. *Biomedical optics: principles and imaging*. John Wiley & Sons, 2012.
29. Sainter AW, King TA, Dickinson MR. Effect of target biological tissue and choice of light source on penetration depth and resolution in optical coherence tomography. *J Biomed Opt* 2004;9:193—9.
30. Rajpoot N, Nayak A, Nayak R, Bankur PK. Evaluation of variation in the palatal gingival biotypes using an ultrasound device. *J Clin Diagn Res* 2015;9:ZC56—60.
31. Furtak A, Leszczynska E, Sender-Janeczek A, Bednarz W. The repeatability and reproducibility of gingival thickness measurement with an ultrasonic device. *Dent Med Probl* 2018;55:281—8.
32. Claffey N, Shanley D. Relationship of gingival thickness and bleeding to loss of probing attachment in shallow sites following nonsurgical periodontal therapy. *J Clin Periodontol* 1986;13:654—7.
33. Anderegg CR, Metzler DG, Nicoll BK. Gingiva thickness in guided tissue regeneration and associated recession at facial furcation defects. *J Periodontol* 1995;66:397—402.
34. Hwang D, Wang HL. Flap thickness as a predictor of root coverage: a systematic review. *J Periodontol* 2006;77:1625—34.
35. Baldi C, Pini-Prato G, Pagliaro U, et al. Coronally advanced flap procedure for root coverage. Is flap thickness a relevant predictor to achieve root coverage? A 19-case series. *J Periodontol* 1999;70:1077—84.
36. Kao RT, Fagan MC, Conte GJ. Thick vs. thin gingival biotypes: a key determinant in treatment planning for dental implants. *J Calif Dent Assoc* 2008;36:193—8.
37. Shao Y, Yin L, Gu J, Wang D, Lu W, Sun Y. Assessment of periodontal biotype in a young Chinese population using different measurement methods. *Sci Rep* 2018;8:11212.